BMC Oral Health

RESEARCH

Open Access

# Finite element analysis of a new alveolar bone splitting technique in the mandibular posterior region

Ye Tian[1], Xiaolu Shi[1], Shaobo Zhai[1], Yang Liu[1], Zheng Yang[1], Yuchuan Wu[1] and Shunli Chu[1*]

## Abstract

**Background** Finite element analysis was used to predict the risk of bone plate fracture and the expected bone augmentation effect of a new alveolar bone splitting technique in the mandibular posterior region for different alveolar crest widths, different alveolar bone densities, different root incision widths, and different insertion depths of bone expansion instrumentation.

**Methods** The jaw models of the mandibular posterior region were constructed by computer-aided software and surgical incisions and bone expansion instruments were prepared on the models, after which the alveolar bone splitting procedure was simulated by finite element analysis software, and the equivalent stress-strain distribution characteristics of the jaw models of each group, as well as the maximal force and the maximal displacement of the bone plate when it was fractured, were recorded.

**Results** The distribution of equivalent stress and strain was mainly concentrated in the cancellous bone area at the root incision and the lower 1/3 of the buccal cortical bone plate, and there was no significant difference in the stress-strain distribution characteristics of the jaw models of each group. The wider of the alveolar crest, the higher the force required to fracture the bone plate, but the smaller the maximum displacement; the plastic deformation capacity of type IV bone jaws was more excellent; the wider the width of the root incision, the shallower the depth of instrument insertion, and the larger the maximum displacement.

**Conclusion** Finite element analysis can effectively simulate the surgical criticality index of the new alveolar bone splitting procedure. Alveolar crest width, alveolar bone density, root incision width, and instrument insertion depth had a clear correlation with the maximum displacement of the bone plate at fracture. The alveolar crest width and alveolar bone density also had a significant effect on the maximum force required to fracture the bone plate.

**Keywords** Alveolar bone splitting, Finite element analysis, Biomechanics, Bone augmentation, Mandible, Oral implants

*Correspondence:
Shunli Chu
chusl@jlu.edu.cn
[1]Department of Implantology, Hospital of Stomatology, Jilin University, Changchun, China

## Introduction

Adequate width and height of alveolar bone are essential for ideal functional reconstruction and aesthetic recovery through implant restoration [1]. However, insufficient alveolar bone width is very common in oral implant surgery, which is related to bone resorption after tooth extraction, periodontal disease, tooth trauma and other factors. It is reported that the bone resorption of alveolar bone after tooth extraction ranges from 29–63% [2]. The mandibular posterior region is an area with weak bone, and the buccal bone plate of the mandible is thinner than the lingual bone plate. Alveolar bone resorption often leads to insufficient horizontal bone mass in the mandibular posterior region. In addition, the mandibular alveolar bone is denser than the maxillary alveolar bone, the blood circulation is relatively poor, and the effect of bone increment is not good. Therefore, how to successfully complete the horizontal bone increment in the mandibular posterior region is a key to implant restoration.

Currently, bone augmentation surgeries commonly used in clinical practice include guided bone regeneration, autologous bone grafting, alveolar bone splitting, distraction osteogenesis, maxillary sinus floor lifting, etc [3]. Among them, alveolar bone splitting is a horizontal bone augmentation procedure suitable for patients with adequate alveolar bone height but insufficient alveolar bone width. Its principle is to longitudinally separate the buccal and lingual bone plates, and use bone expansion tools to move the buccal bone plate to the buccal side, so as to achieve the purpose of horizontal bone augmentation. Traditional alveolar bone splitting is to use a bone splitting instrument to prepare a horizontal bone incision on the top of the alveolar ridge, which penetrates vertically into the cancellous bone, and then make vertical loose bone incisions from both ends of the horizontal bone incision toward the root, deepening into the subcortical bone, followed by bone splitting, bone compression and bone expansion. The bone augmentation effect of this surgery is obvious, and it can be widely used for thin alveolar bone after maxillary and mandibular dentition defects and dentition loss. The key to the success of traditional alveolar bone splitting surgery is to avoid bone plate fracture and ensure blood supply. However, compared with the more elastic maxilla, the alveolar bone in the mandibular posterior region is more mineralized and less tough, and the bone plate is prone to fracture during bone expansion. Although “two-stage [4] " or “three-stage [5] " bone splitting surgery can be adopted, it also prolongs the treatment time and increases the risk of bone resorption.

In recent years, more and more scholars have improved alveolar bone splitting surgery to make it more widely applicable and reduce the incidence of complications. For example, Blus and Szmukler et al. [6] added a longitudinal incision at the bottom of the mandibular alveolar bone, aiming to create a hinge effect during the alveolar bone splitting process, thereby reducing the risk of fracture. Marcello et al. [7] prepared a rectangular incision to disconnect or partially disconnect the buccal bone plate, and then used steel wire ligation and fixation to obtain good initial stability of the implant. Inspired by Blus et al., this research team also designed a new alveolar bone splitting technique. The principle of this technique is to use an ultrasonic osteotome to perform traditional alveolar bone splitting, and then prepare a horizontal incision that only cuts through the cortical bone at the bottom of the mandible and between the vertical incisions. Afterwards, the bleeding holes are prepared on the surface of the buccal bone plate to ensure blood supply, and then combined with guided bone regeneration to guarantee the bone augmentation effect. Our team has applied it to many cases of insufficient width of mandibular alveolar bone, which have safely and effectively increased the width of alveolar bone in the surgical area, and achieved ideal repair results.

This paper describes a novel alveolar bone splitting technique applied to the mandibular posterior region. Although this technique has achieved satisfactory results in clinic, whether it is this technique or other modified alveolar splitting techniques, in the course of clinical operation, implant doctors often rely on their own experience or feel to perform bone splitting and bone expansion operations. Without sufficient systematic theoretical guidance, it is difficult to predict the timing of bone plate fracture. In light of this situation, the maximum extent of expansion and fracture time of the bone plate are examined through simulating alveolar bone splitting, with finite element analysis offering unparalleled advantages [8]. Based on this, this study utilized computer-aided design software to construct a mandibular posterior region jaw model, followed by finite element analysis software to investigate: (1) the impact of varying alveolar crest widths on the new alveolar bone splitting technique; (2) the influence of different alveolar bone densities on the new alveolar bone splitting technique; (3) the effect of incision widths at the root of alveolar bone on the new alveolar bone splitting technique; and (4) the influence of different insertion depths of bone expansion instruments on the new alveolar bone splitting technique. The present study employed finite element analysis to simulate the new alveolar bone splitting technology, aiming to investigate the anticipated effect on bone augmentation and critical fracture index of this technique under diverse clinical conditions. By addressing the limitation of relying solely on clinical experience for bone expansion, this research provides a systematic theoretical foundation for horizontal bone increment technology and offers practical guidance for its clinical application.

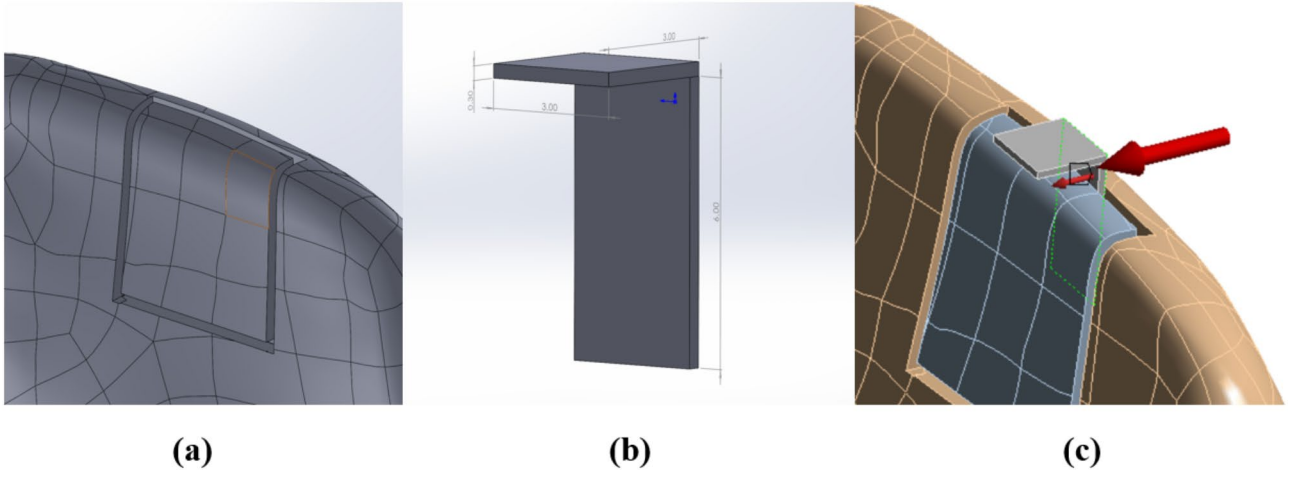


**Fig. 1** Schematic diagram of finite element analysis model. (**a**) Four surgical incisions; (**b**) Model dimensions of bone expansion instruments; (**c**) The direction of force exerted

## Materials and methods

### Establishment of jaw model

A volunteer with complete mandibular dentition and no history of periodontitis and jaw disease was selected to take the cone beam computed tomography (CBCT) (Carestream Health, Inc., Canada) of the jaw. After the CBCT images were stored in DICOM format, the jaw model of the mandibular posterior region was extracted by Mimics21.0 software (Materialise, Inc., Belgium) and saved in STL format. The jaw model was imported into GeomagicWrap2017 software (3DSystems, Inc., USA) to optimize, smooth and trim the model. The jaw model with cortical bone thickness of 1 mm and 2 mm was constructed by offset function, and the jaw model with alveolar crest width of 3 mm and 4 mm was constructed by resection function and saved in STP format (Fig.S1).

### Construction of surgical incision and bone expansion instrument model

The model data from step 2.1 were imported into Solidworks2022 software (Dassault Systemes, Inc., USA), and four incisions for new alveolar bone splitting technique were made on each group of jaw models (Fig. 1). The width of the incision at the bottom of the alveolar bone was set to 0.5 mm and 1.0 mm and 1.5 mm respectively (Fig.S1). The bone expansion instrument model was constructed through the sketch function (Fig. 1). The length of the contact part between the instrument model and the jaw was set as 3 mm, 5 mm, 7 mm respectively (Fig.S1). After that, the instrument model and the jaw model were assembled and saved in STEP format.

### Setting of finite element analysis parameters

The model data from step 2.2 were imported into Workbench 22.0 software (Ansys, Inc., USA), and the transient structural analysis module was applied to enter the modulus of elasticity and Poisson's ratio of each material and assign values (Table 1) [9–11]. All materials in the experiment were set to be isotropic and homogeneous. The contact relationship between each component of the model was set to a "Bonded" connection, and the contact tolerance was defined as 0.1 mm. Tetrahedral mesh elements were utilized for free mesh subdivision. Based on the results of convergence testing (Tab. S1), a mesh size of 0.5 mm was chosen for the jaw model, while a size of 0.2 mm was selected for the instrument model. The final number of mesh elements and nodes for each jaw model were presented in Table 2. The jaw model surrounding the surgical incision was immobilized, and a vector force was applied orthogonally to the surface of the expansion instrument, with its magnitude increasing linearly over time (Fig. 1). Throughout the movement of the expansion instrument, the direction of force remains consistently perpendicular to its surface. The total degree of deformation, equivalent force and equivalent strain of each group of models reaching the ultimate yield state were finally solved, and the trend of the distribution of equivalent force and strain of each group was recorded, as well as the maximum force and the total degree of deformation in the ultimate yield state. Referring to the literature of other scholars [12–16], in this study, 50 MPa was used as the ultimate shear strength of cortical bone, 10 MPa was

**Table 1** Physical properties of materials used in the experiment

| Materials | Modulus of elasticity (GPa) | Poisson's ratio | Density (g/cm$^3$) |
|---|---|---|---|
| Cortical bone | 13.4 | 0.30 | 2.10 |
| Dense cancellous bone (type I, II, III bone) | 1.37 | 0.30 | 1.80 |
| Loose cancellous bone (type IV bone) | 1.10 | 0.30 | 1.60 |
| Structural steel | 200.00 | 0.30 | 7.85 |

**Table 2** Results of finite element analysis of jaw models in each group

| Model | Alveolar crest width (mm) | Alveolar bone density (type II、III、IV bone) | Root incision width (mm) | Insertion depth of instrument model (mm) | Elements | Maximum force (*N*) | Maximum displacement (mm) |
|---|---|---|---|---|---|---|---|
| M1 | 3 | III | 0.5 | 5 | 442,517 | 25 | 0.65 ± 0.09 |
| M2 | 4 | III | 0.5 | 5 | 520,959 | 90 | 0.44 ± 0.13 |
| M3 | 3 | II | 0.5 | 5 | 431,519 | 6 | 0.60 ± 0.06 |
| M4 | 3 | IV | 0.5 | 5 | 442,517 | 30 | 0.88 ± 0.13 |
| M5 | 3 | III | 1.0 | 5 | 442,400 | 25 | 0.76 ± 0.11 |
| M6 | 3 | III | 1.5 | 5 | 442,414 | 25 | 0.89 ± 0.14 |
| M7 | 3 | III | 0.5 | 3 | 434,362 | 25 | 0.77 ± 0.12 |
| M8 | 3 | III | 0.5 | 7 | 434,962 | 25 | 0.56 ± 0.08 |

used as the ultimate shear strength of cancellous bone, and 2% strain rate was used as the yield strain of cortical bone and cancellous bone. In this case, 10 locations were randomly selected at the top of the alveolar ridge of the jaw model, and the average value of their total degree of deformation was taken as the maximum displacement when the jaw model reached the ultimate yield state.

### Statistical analysis

Data analysis and figure construction was performed using GraphPad Prism 6 (GraphPad, San Diego, USA). Values represent mean ± standard deviation (SD). Comparison among different groups was made by two-way analysis of variance (ANOVA). $P$ values < 0.05 were considered statistically significant.

## Results

The experimental jaw model consisted of three main parts: external cortical bone, free cortical bone and cancellous bone. Considering the shear strength and yield strain of cortical bone and cancellous bone, in the cancellous bone model, the parts with an equivalent stress of 10 MPa or less were set in blue; in the cortical bone model, the parts with an equivalent stress of 50 MPa and 10 MPa or less were set in light blue and blue; and the parts with a strain rate of 2% or less were set in blue.

Among the indicators that the jaw model reached the ultimate yield state was when the buccal and lingual cancellous bone at the root incision appeared to have a phase-continuous distribution of equivalent stresses that exceeded the ultimate shear strength of the cancellous bone and a significant distribution of equivalent strains that exceeded their yield strains at the cancellous bone on both sides. The experimental results were shown in Table 2; Fig. 2.

There was no significant difference in the distribution characteristics of equivalent stress and strain in each part of each model. Taking M1 as an example, the results of the equivalent stress and equivalent strain distribution of its various parts were shown in Fig. 3. As could be seen from the figure, the equivalent stress and equivalent strain of the cancellous bone model were mainly concentrated in the cancellous bone region at the root-square incision, and the distribution range of the equivalent stress-strain was gradually expanded with the increase of the acting force. The equivalent stress-strain distribution of the cancellous bone on the lingual side was more extensive than that on the buccal side, while the equivalent stress-strain magnitude of the cancellous bone on the buccal side was higher than that on the lingual side. The equivalent strains exceeding the yield strain of the cancellous bone first appeared in the area of cancellous bone on both sides of the root-square incision, and gradually spread from the two sides to the middle as the value of the force increased.

The equivalent stresses in the buccal free cortical bone first appeared in the lower 1/3 of the bone plate, and as the value of the force increased, the distribution of the equivalent stresses gradually approached to the lower edge of the buccal bone plate. The equivalent stresses in the lingual free cortical bone first appeared at the cutting angle on both sides of the bone plate, and as the value of the applied force increased, the equivalent stresses were gradually distributed all over the lower edge of the lingual plate, and also appeared in the lower 1/3 of the lingual bone plate as well as at the top of the alveolar crest. The equivalent stress distribution in the external cortical bone was located at the lower edge of the surgical incision at the buccal and lingual lateral bone plates. The equivalent strains of free and external cortical bone did not change significantly and were much less than 2% in all groups of models. In addition, M3 did not show significant equivalent stress-strain changes in free cortical bone and external cortical bone because the maximum force was too small.

## Discussion

The clinical cases with insufficient horizontal bone for implant restorative treatment must undergo bone augmentation surgery prior to implantation. In addition to classical guided bone regeneration and autologous bone grafting, alveolar bone splitting, which can effectively

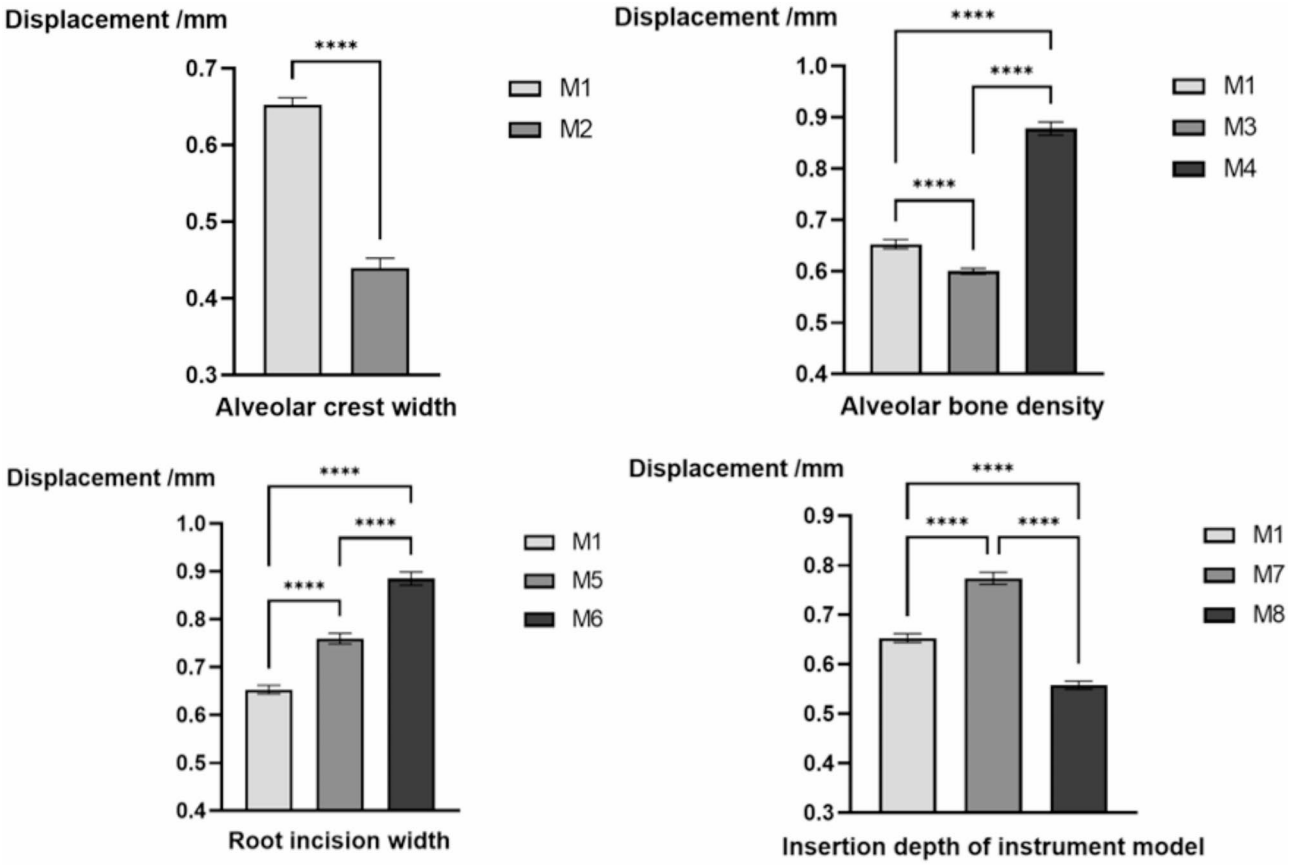


**Fig. 2** The maximum displacement results of finite element analysis of jaw models in various groups. Note: *, $P<0.05$; ****, $P<0.001$

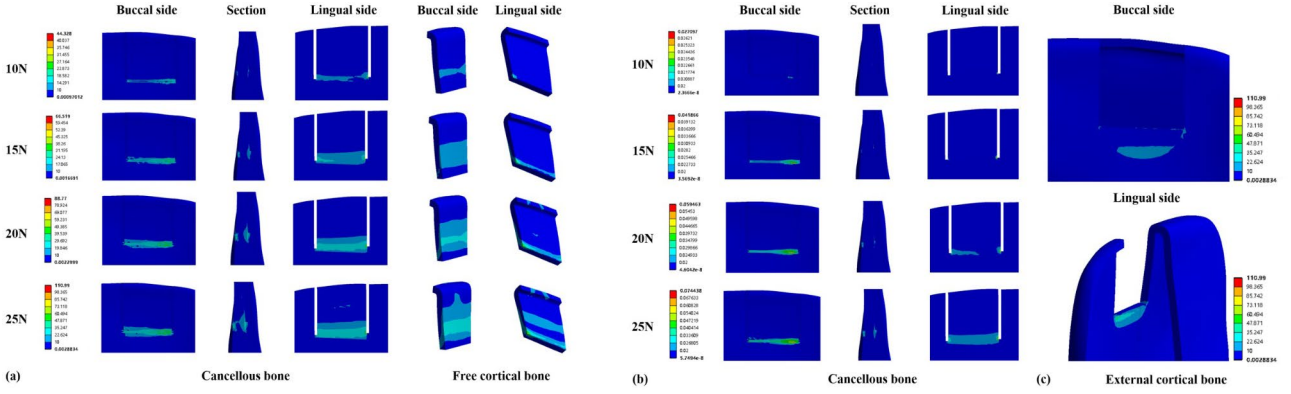


**Fig. 3** Distribution characteristics of equivalent stress and equivalent strain of M1. (**a**) Equivalent stress distribution characteristics of cancellous bone and free cortical bone; (b) Equivalent strain distribution characteristics of cancellous bone; (**c**) Equivalent stress distribution characteristics of external cortical bone

increase the horizontal alveolar bone width, is an ideal option [17, 18]. However, when the alveolar bone is heavily resorbed, the brittleness of the buccal bone plate increases, especially the buccal alveolar bone in the mandibular posterior region, which greatly increases the risk of fracture of the bone plate during bone expansion by alveolar bone splitting. The risk of alveolar bone splitting complications can be reduced by preoperatively predicting the stress-strain distribution of the bone plate during expansion [8]. In order to predict the risk of bone plate fracture for the new alveolar bone splitting technique, an in-depth understanding of the expansion behaviour of the buccal bone plate and insight into its fracture mechanism is essential. In this context, finite element analysis can provide sufficient tools to analyze the principles of bone plate fracture in the new alveolar bone

splitting technique. Finite element analysis of alveolar bone splitting has not been extensively conducted in the biomedical field, and this study represents the first report on research regarding this innovative technique.

Studies have shown that retaining at least 3 mm of alveolar bone width and a minimum vertical bone height of 10 mm is necessary to provide sufficient buccal and lingual cortical and cancellous bone volume to maintain adequate blood supply to the bone adjacent to the implant, thus ensuring the success of alveolar bone splitting [1, 19]. Based on this, considering that fine-diameter implants can be selected for implant restorations in clinical work when facing clinical patients with a residual bone width of up to 5 mm, the jaw bone models with 3 mm alveolar crest width and 4 mm alveolar crest width were constructed for finite element analysis in this study. Theoretically, after removing 1 mm of cortical bone, the width of the cancellous bone at the root incision of the 4 mm jaw model is thicker compared to that of the 3 mm jaw model, and thus it can withstand a higher external force before reaching the ultimate yield state. The experimental results shown that the maximum force of the 4 mm jaw model was 90 N, while the maximum force of the 3 mm jaw model was 25 N. The findings suggest that in clinical practice, when dealing with alveolar crest width less than 3 mm, it is advisable for clinicians to limit the applied force for bone expansion to no more than 25 N in order to minimize the risk of buccal bone plate fracture. Unexpectedly, the distribution range of equivalent stress and equivalent strain in the 4 mm jaw model was wider than that of the 3 mm jaw model under higher forces, which meant that the area exceeding the shear strength and yield strain was larger, and the range of plastic deformation was wider in the 4 mm jaw model. This means that the 4 mm jaw model has a larger area above the shear strength and yield strain, and a wider range of plastic deformation. Therefore, it was easier for the 4 mm jaw model to reach the ultimate yield state. The results of the total deformation degree also proved this point. In the ultimate yielding state, the displacement of the 4 mm jaw model at the top of the alveolar ridge was $0.44 \pm 0.13$ mm, which was less than that of the 3 mm jaw model ($0.65 \pm 0.09$ mm). Admittedly, this result falls significantly short of the horizontal alveolar bone augmentation of $1.19 \pm 1.01$ mm achieved through alveolar bone splitting in Bassctti et al.'s study [20]. Moreover, it is anticipated that the new technique of alveolar bone splitting will yield a far greater effect on bone augmentation in actual clinical scenarios. In addition to theoretical errors in finite element analysis, the primary reason lies in the exclusive influence of alveolar bone type factors on the maximum displacement observed in this study, without considering biogenic osteogenesis or other bone augmentation factors such as GBR. The significance of this measure primarily lies in reflecting the anticipated trend of bone augmentation size, indicating that patients with a narrow alveolar crest may experience a greater effect on bone augmentation compared to those with a wide alveolar crest. Besides, it could be found that the equivalent stress and equivalent strain distributions were inconsistent when the jaw model was in the ultimate yielding state. For example, when the 3 mm jaw model was in the ultimate yielding state, the buccal and lingual cancellous bone at the root incision had already experienced equivalent stress continuity, but the equivalent strains were still distributed only in the superficial layers of the buccal and lingual cancellous bone; when the equivalent stress at the edge of the free cortical bone had already exceeded the shear strength, the corresponding equivalent strain exceeding the yield strength was not observed, which may be related to the phenomenon of "hysteresis" [21] in osteo-viscoelasticity, where the strain response lags behind the stress. It is worth noting that during bone expansion, the stresses and strains were more concentrated in the cancellous bone and external cortical bone located in the region of the root incision, as well as in the lower 1/3 of the buccal lamellae of the free cortical bone, which suggests that in some cases of thin cortical bone, as the force increases, the buccal lamellae breakage may be located in the lower 1/3 of the lamellae, in addition to occurring in the root incision location. The discovery might serve as a reminder for doctors to safeguard the buccal bone plate's underside during bone expansion procedures, such as employing manual pressure against the buccal bone plate.

As mentioned previously, thin cortical bone has an effect on the fracture location of bone plate. Duttenhoefer et al. [22] also found that the fracture lines were mostly located in the weakest area of the bone plate locally through the alveolar bone splitting experiments on human jawbone specimens. Based on this, this study constructed jaw bone models with four bone densities according to the Lekholm-Zarb bone density classification, but only finite element analyses were carried out on the type II, III and IV bone jaw bone models in consideration of practical clinical applications. The maximum forces in the type II, III, and IV bone jaw models differed considerably after the removal of the underlying cortical bone. In the type II bone model, only a few cancellous bones remained to maintain the jaw morphology after the removal of the 2 mm thickness of cortical bone, and the type II bone model reached the ultimate yield state at a very low force, taking into account the lower shear strength of cancellous bone. The aforementioned statement aligns with the findings of Stricker et al. [23], indicating that fractures in bone plates are primarily associated with the thickness of the underlying basal bone. The implication of this is that in patients with type

II bone, it is not feasible to completely excise all the cortical bone from the surface of the buccal bone plate during new alveolar bone splitting technique, in order to prevent abrupt fracture of the buccal bone plate.

At the root incision, the difference between the type II bone model and the type III bone model only lay in the thickness of the cancellous bone, so the equivalent stress-strain distribution characteristics of the two were not significantly different. Because of the low maximum force, the type II bone model did not show significant equivalent stress-strain distribution in the free cortical bone and external cortical bone.

In addition, the difference between the type III and IV bone models is only reflected in the physical property parameters of the internal cancellous bone, so there is no significant difference in the equivalent stress-strain distribution characteristics between the two models. Additionally, the disparity between the type III and IV jaw models solely manifested in the physical parameters of the internal cancellous bone. As cancellous bone density increased, there was a slight reduction in the range of equivalent stress-strain distribution; however, no significant difference was observed, aligning with Ghosh et al.'s findings [24].

The total deformation results of the jaw models with different alveolar bone density indicated that the maximum displacement of the type II bone model was $0.60 \pm 0.06$ mm, which aligned closely with the findings reported by Stricker et al. [23], who conducted an alveolar bone splitting experiment on pig jaw models. Based on CT data, it was observed that the density of the pig jaw resembled that of type II bone. The plastic deformation of cancellous bone approached its limit when the displacement of the bone plate reached approximately 0.6 mm. The type II bone model exhibits the lowest maximum displacement, which could potentially be attributed to the narrow remaining cancellous bone width at the root incision. There was a significant difference in the maximum displacement between the type III and IV bone models, indicating that there is an effect of different physical parameters of cancellous bone on the degree of deformation, which may be related to the fact that cancellous bone is a highly functionally compliant tissue. The plastic deformation of cancellous bone in studies related to total ankle arthroplasty is predominantly influenced by the specific plastic formula employed [25–27]. The results of this study suggest that lax cancellous bone may possess more excellent plastic deformation ability than dense cancellous bone. This is in line with the majority of research findings, which suggest that greater bone flexibility reduces the likelihood of buccal bone plate fracture during expansion [28, 29]. Conversely, higher bone density correlates with increased brittleness and a heightened risk of fracture.

The improvement of the new alveolar bone splitting technique lies in the new root incision between the vertical incisions on both sides. At this position, when the cortical bone on the surface of the buccal bone plate is removed, only the cancellous bone is retained to maintain the continuity of the bone plate. The area of cancellous bone uncovered by cortical bone varies according to the width of the root incision, which is certainly a critical factor in alveolar bone splitting, which relies primarily on the ability of cancellous bone to deform plastically for bone expansion. Based on this, this study constructed 0.5 mm incision, 1.0 mm incision, and 1.5 mm incision jaw models to investigate whether there is any effect on the bone augmentation effect of the new alveolar bone splitting technique. The maximum force exerted by the three jaw models was 25 N, suggesting that the factors influencing bone plate fracture appeared to be independent of the exposed cancellous bone area. The results of equivalent stress-strain distribution characteristics showed that the area of cancellous bone without cortical bone coverage increased with increasing incision width, and the wider incision model had a wider range of equivalent stress-strain distribution under the same value of acting force. The comprehensibility of this statement is apparent, however, it is noteworthy that the maximum displacement of each jaw model gradually increased with the increase of the root incision width after reaching the ultimate yield state, which implies that the larger the area of the cancellous bone region without cortical bone coverage, the greater the plastic deformation capacity under the same cancellous bone physical property parameters. The principle is actually quite straightforward. For instance, when using a ruler, we secure one end of it to the table and then, before breaking the ruler, grasp the other end and vigorously shake it. Evidently, the longer the ruler is, the greater our capacity for shaking. However, in the current clinical scenario, it is not feasible to extensively remove cortical bone from the patient's buccal bone plate in order to achieve a more pronounced effect on bone increment. Undoubtedly, maintaining a delicate balance between the extent of cortical bone removal and creating an optimal environment for bone regeneration poses a novel challenge.

The bone expansion principle of the new alveolar bone splitting is to prepare the root cortical bone incision and make use of the adaptability and plasticity of cancellous bone to reduce the risk of cortical bone fracture. During bone expansion, the buccal bone plate is rotated by the acting force of the bone expansion instrument, using the inner edge of the root incision as the fulcrum. If the distance between the bone expansion instrument and the root incision is farther, which corresponds to the longer power arm, the greater the stress at the root incision under the same force conditions. Based on this, the

jaw models of 3 mm depth, 5 mm depth and 7 mm depth were constructed to explore the effect of new alveolar bone splitting technique with different depth of bone expansion instruments. The experimental results demonstrated that there was no significant difference in the equivalent stress-strain distribution characteristics of the 3 mm depth, 5 mm depth, and 7 mm depth jaw models, but the magnitude of the equivalent stresses in each jaw model under the same force gradually decreased with the increase of the insertion depth of the instrumented model, which was consistent with the previous hypothesis. There was no difference in the maximum force in the jaw models with different instrument insertion depths, indicating that the distance between the instrumented model and the root incision was not sufficient in the jaw models to affect a change in the value of the force that would bring the cancellous bone to its ultimate yield state. However, the maximum displacement of the jaw models with different instrument insertion depths decreased with increasing insertion depth, indicating that the deeper the insertion depth, the larger the contact area between the instrumented model and the cancellous bone, and the smaller the pressure borne by the cancellous bone per unit area under the same acting force, i.e., the lower the stress. In a low stress state, the ability of cancellous bone to deform plastically may be limited. We hypothesize that this phenomenon may be attributed to microdamage in cancellous bone. The elastic modulus of cancellous bone experiences a significant decrease once it surpasses the yield strength, as the internal structure of cancellous bone undergoes slight cracking [30, 31]. Relevant research indicates that microdamage occurs at approximately 1.6% tissue strain, with a lower threshold for occurrence in finite element analysis models [32, 33]. The presence of microdamage allows certain tissue levels to be high enough to induce local yielding and a concomitant decline in whole-specimen properties, even at low magnitudes of apparent stress [34, 35]. Moreover, an increase in force area leads to a greater occurrence of microdamage areas, resulting in a more pronounced reduction in the overall modulus of cancellous bone and further constraining its plastic deformation ability. Interestingly, this may contradict our conventional understanding that a larger stress area leads to a more uniform stress distribution and reduces the likelihood of bone plate fracture. However, it could be true that in order to achieve optimal bone augmentation effect, minimizing the stress area of the bone plate is necessary, such as by using a thinner bone dilator or inserting it at a shallower depth for dilation.

It is very difficult to map the bone expansion mechanism and stress distribution of the new alveolar bone splitting technique in clinical practice. Hence, for exploring the theoretical basis of the technique, biomechanical analysis tools are needed. To date, finite element analysis is a commonly used tool in mechanics and biomechanics virtual analysis of mechanical strength and stress shielding [36], among others, and its emergence has provided new ideas and solutions to study the bone plate fracture mechanism of alveolar bone splitting. In this experiment, the influence of four factors, namely, alveolar crest width, alveolar bone density, surgical incision width, and instrument insertion depth, on the bone augmentation effect of the new alveolar bone splitting technique was investigated by means of finite element analysis, and the corresponding results were obtained. Nevertheless, there are still some limitations and need to be improved in the course of this study, and the shortcomings are as follows.

The parameter settings of the research model are not reasonable enough. It is well known that cortical bone and cancellous bone have biomechanical properties such as anisotropy and non-homogeneity. However, in this study, the cortical bone and cancellous bone were set to be isotropic and homogeneous in order to facilitate the calculation. The change in material properties will undoubtedly affect the accuracy of the experimental results. Differential material assignment can be considered through the grey value of the CBCT image of each mesh element in the model to obtain an anisotropic, non-homogeneous jaw model [37–39].

The research on the basis of system theory was not thorough enough. Although this study investigated the effects of four different factors on the new alveolar bone splitting technique to explore the theoretical basis of the technique, it was not thorough enough. Mainly reflected in: (1) Alveolar bone splitting, as a bone augmentation method, is also affected by its subsequent treatment process, such as implant placement, which also extrudes the buccal bone plate and further expands the width of alveolar bone. Therefore, it can be considered to add the implant implantation process to the subsequent research process, so as to analyze the influence of the new alveolar bone splitting on the bone augmentation effect of implant restorations in a more complete way. (2) In this experiment, the study subjects were various jaw models that underwent only the new alveolar bone splitting procedure, and the control group was missing. In order to reflect the changes in the improved alveolar bone splitting technique, finite element analysis of the traditional alveolar bone splitting technique could be added to explore the shortcomings of the new alveolar bone splitting technique through a comparative study so that the technique can be further improved. (3) There are more variables in alveolar bone splitting than the four factors studied in this experiment, such as the depth of the surgical incision, the thickness of the bone plate at the base of the jaw, etc., and the corresponding jaw models can

be constructed for the finite element analysis in order to improve the theoretical basis of this technique.

There is a discrepancy between finite element theoretical analysis and real practice. Simple jaw models can accurately predict the timing and location of bone plate fracture through finite element analysis, but the human jaw is not only a biomaterial with complex mechanical properties, but also a biological organ that carries mechanical loads, and the growth and development of cells and metabolism will lead to changes in the quantity and quality of the jawbone, which will affect its complex mechanical properties. Furthermore, the thicknesses of cortical bone and cancellous bone in the various jaw models in this study were relatively fixed, while the thicknesses of cortical bone and cancellous bone in human jaws in real life are varied and not uniform. Although the material parameters and deformation conditions are set reasonably, further basic research is still needed to prove the accuracy of the finite element modelling theory, and only by combining the theory with practice can the theoretical basis of the technique be truly formed.

## 5 Conclusion

This experiment investigated the finite element analysis of a new alveolar bone splitting technique under four different factors. The results showed that, among the jaw models with different alveolar crest widths, the wider the alveolar crest, the higher the maximum force to reach the ultimate yield state, but the smaller the maximum displacement at the alveolar crest at that state; among the jaw models with different alveolar bone densities, the maximal force and the maximal displacement to reach the ultimate yield state of the jaw model of type II bone were the smallest and the plastic deformation ability of the jaw model of type IV bone was more excellent because of its loose cancellous bone; among the jaw models with different root incision widths, the wider the root incision, the larger the area of cancellous bone without cortical bone coverage, and the larger the maximum displacement at ultimate yield; among the jaw models with different insertion depths of bone expansion instruments, the deeper the insertion of the instruments, the lower the stresses, and the lower the maximum displacement at ultimate yield under the same force. Regardless of the type of jaw model, the main concentration of stress and strain was at the root incision, followed by the lower 1/3 of the buccal bone plate, and with the increase of the value of the force, the lower edge of the instrumented model also showed a concentration of stress.

## Supplementary Information

The online version contains supplementary material available at https://doi.org/10.1186/s12903-025-05559-5.

Supplementary Material 1: **Fig. S1.** Schematic diagram of each jaw model: (a) M1 jaw model with 3 mm alveolar crest width and M2 with 4 mm alveolar crest width; (b) M3 with type II of alveolar bone density, M1 with type III of alveolar bone density and M4 with type IV of alveolar bone density; (c) M1 with 0.5 mm root incision width, M5 with 1.0 mm root incision width and M6 with 1.5 mm root incision width; (d) M7 with 3 mm insertion depth of instrument model, M1 with 5 mm insertion depth of instrument model and M8 with 7 mm insertion depth of instrument model.

Supplementary Material 2: **Tab. S1**. The convergence test results for the division of mesh size.

**Acknowledgements**
We thank Liwen Bianji (Edanz) (www.liwenbianji.cn) for editing the language of a draft of this manuscript.

**Author contributions**
Y. T. led the writing and did most of the experiments. S. C. critically revised the manuscript. X. S., S. Z. and Y. L. analyzed the experimental data. Z. Y. and Y. W. contributed to charting. Every author gave final approval and agreed to be accountable for all aspects of the work.

**Funding**
This work was supported by the Science and Technology Development Project of Jilin Provincial Department of Science and Technology, China (Grant No. 20230203065SF).

**Data availability**
No datasets were generated or analysed during the current study.

## Declarations

**Ethics approval and consent to participate**
Not applicable.

**Consent for publication**
Not applicable.

**Competing interests**
The authors declare no competing interests.

Received: 25 April 2024 / Accepted: 27 January 2025
Published online: 08 March 2025

**References**

1. Starch-Jensen T, Becktor JP. Maxillary Alveolar Ridge Expansion with Split-Crest technique compared with lateral Ridge Augmentation with Autogenous Bone Block Graft: a systematic review. J Oral Maxillofac Res. 2019;10(4):e2.
2. Tan WL, Wong TL, Wong MC, Lang NP. A systematic review of post-extractional alveolar hard and soft tissue dimensional changes in humans. Clin Oral Implants Res. 2012;23(Suppl 5):1–21.
3. Tolstunov L, Hamrick JFE, Broumand V, Shilo D, Rachmiel A. Bone augmentation techniques for Horizontal and Vertical Alveolar Ridge Deficiency in oral implantology. Oral Maxillofac Surg Clin North Am. 2019;31(2):163–91.
4. Edranov SS, Matveeva NY, Kalinichenko SG. Evaluation of the effectiveness of bone grafting in Alveolar Ridge Augmentation using the two-stage splitting technique. Bull Exp Biol Med. 2023;176(2):268–74.
5. Hu GH, Froum SJ, Alodadi A, Nose F, Yu YP, Suzuki T, Cho SC. A Three-Stage Split-Crest technique: Case Series of Horizontal Ridge Augmentation in the atrophic posterior mandible. Int J Periodontics Restor Dent. 2018;38(4):565–73.
6. Blus C, Szmukler-Moncler S. Split-crest and immediate implant placement with ultra-sonic bone surgery: a 3-year life-table analysis with 230 treated sites. Clin Oral Implants Res. 2006;17(6):700–7.
7. Contessi M. The monocortical window (MCW): a modified split-crest technique adopting ligature osteosynthesis. Int J Periodontics Restor Dent. 2013;33(6):e127–139.

8. Çelebi Bektaş A, Yalçın M. Evaluation of deformation in the buccal lamellar bone with finite element analysis in alveolar ridge-splitting/expansion technique. J Stomatol Oral Maxillofac Surg. 2021;122(6):578–82.
9. Chang SH, Lin CL, Hsue SS, Lin YS, Huang SR. Biomechanical analysis of the effects of implant diameter and bone quality in short implants placed in the atrophic posterior maxilla. Med Eng Phys. 2012;34(2):153–60.
10. Silva LS, Verri FR, Lemos CAA, Martins CM, Pellizzer EP, de Souza Batista VE. Biomechanical effect of an occlusal device for patients with an implant-supported fixed dental prosthesis under parafunctional loading: A 3D finite element analysis. *J Prosthet Dent* 2021, 126(2):223.e221-223.e228.
11. Staiger MP, Pietak AM, Huadmai J, Dias G. Magnesium and its alloys as orthopedic biomaterials: a review. Biomaterials. 2006;27(9):1728–34.
12. Turner CH, Wang T, Burr DB. Shear strength and fatigue properties of human cortical bone determined from pure shear tests. Calcif Tissue Int. 2001;69(6):373–8.
13. Brown AD, Rafaels KA, Weerasooriya T. Shear behavior of human skull bones. J Mech Behav Biomed Mater. 2021;116:104343.
14. McElhaney JH, Fogle JL, Melvin JW, Haynes RR, Roberts VL, Alem NM. Mechanical properties on cranial bone. J Biomech. 1970;3(5):495–511.
15. Halawa M, Lee AJ, Ling RS, Vangala SS. The shear strength of trabecular bone from the femur, and some factors affecting the shear strength of the cement-bone interface. Arch Orthop Trauma Surg (1978). 1978;92(1):19–30.
16. Linde F, Hvid I, Pongsoipetch B. Energy absorptive properties of human trabecular bone specimens during axial compression. J Orthop Res. 1989;7(3):432–9.
17. Issa DR, Elamrousy W, Gamal AY. Alveolar ridge splitting and simvastatin loaded xenograft for guided bone regeneration and simultaneous implant placement: randomized controlled clinical trial. Clin Oral Investig. 2024;28(1):71.
18. Lin Y, Li G, Xu T, Zhou X, Luo F. The efficacy of alveolar ridge split on implants: a systematic review and meta-analysis. BMC Oral Health. 2023;23(1):894.
19. Jha N, Choi EH, Kaushik NK, Ryu JJ. Types of devices used in ridge split procedure for alveolar bone expansion: a systematic review. PLoS ONE. 2017;12(7):e0180342.
20. Bassetti R, Bassetti M, Mericske-Stern R, Enkling N. Piezoelectric alveolar ridge-splitting technique with simultaneous implant placement: a cohort study with 2-year radiographic results. Int J Oral Maxillofac Implants. 2013;28(6):1570–80.
21. Wu B, Wu Y, Liu M, Liu J, Jiang D, Ma S, Yan B, Lu Y. Mechanical behavior of human cancellous bone in alveolar bone under Uniaxial Compression and Creep tests. Mater (Basel) 2022, 15(17).
22. Duttenhoefer F, Varga P, Jenni D, Grünwald L, Thiemann L, Gueorguiev B, Stricker A. The Alveolar Ridge Splitting Technique on Maxillae: A Biomechanical Human Cadaveric Investigation. *Biomed Res Int* 2020, 2020:8894471.
23. Stricker A, Widmer D, Gueorguiev B, Wahl D, Varga P, Duttenhoefer F. Finite Element Analysis and Biomechanical Testing to Analyze Fracture Displacement of Alveolar Ridge Splitting. *Biomed Res Int* 2018, 2018:3579654.
24. Kumar A, Mondal S, Ghosh R. Biomechanical performance of the cemented acetabular cup with combined effects of bone quality, implant material combinations and bodyweight. Proc Inst Mech Eng H. 2022;236(9):1309–27.
25. Minku, Mukherjee K, Ghosh R. Assessment of bone ingrowth around beaded coated tibial implant for total ankle replacement using mechanoregulatory algorithm. Comput Biol Med. 2024;175:108551.
26. Mondal S, Ghosh R. Effects of implant orientation and implant material on tibia bone strain, implant-bone micromotion, contact pressure, and wear depth due to total ankle replacement. Proc Inst Mech Eng H. 2019;233(3):318–31.
27. Kelly N, Cawley DT, Shannon FJ, McGarry JP. An investigation of the inelastic behaviour of trabecular bone during the press-fit implantation of a tibial component in total knee arthroplasty. Med Eng Phys. 2013;35(11):1599–606.
28. Scipioni A, Bruschi GB, Giargia M, Berglundh T, Lindhe J. Healing at implants with and without primary bone contact. An experimental study in dogs. Clin Oral Implants Res. 1997;8(1):39–47.
29. Enislidis G, Wittwer G, Ewers R. Preliminary report on a staged ridge splitting technique for implant placement in the mandible: a technical note. Int J Oral Maxillofac Implants. 2006;21(3):445–9.
30. Fyhrie DP, Schaffler MB. Failure mechanisms in human vertebral cancellous bone. Bone. 1994;15(1):105–9.
31. Morgan EF, Unnikrisnan GU, Hussein AI. Bone mechanical properties in Healthy and Diseased States. Annu Rev Biomed Eng. 2018;20:119–43.
32. Goff MG, Lambers FM, Sorna RM, Keaveny TM, Hernandez CJ. Finite element models predict the location of microdamage in cancellous bone following uniaxial loading. J Biomech. 2015;48(15):4142–8.
33. Jungmann R, Szabo ME, Schitter G, Tang RY, Vashishth D, Hansma PK, Thurner PJ. Local strain and damage mapping in single trabeculae during three-point bending tests. J Mech Behav Biomed Mater. 2011;4(4):523–34.
34. Tang SY, Vashishth D. A non-invasive in vitro technique for the three-dimensional quantification of microdamage in trabecular bone. Bone. 2007;40(5):1259–64.
35. Morgan EF, Yeh OC, Keaveny TM. Damage in trabecular bone at small strains. Eur J Morphol. 2005;42(1–2):13–21.
36. Falcinelli C, Valente F, Vasta M, Traini T. Finite element analysis in implant dentistry: state of the art and future directions. Dent Mater. 2023;39(6):539–56.
37. Clarke IC. Role of ceramic implants. Design and clinical success with total hip prosthetic ceramic-to-ceramic bearings. Clin Orthop Relat Res. 1992;282:19–30.
38. Kumar A, Mondal S, Ghosh R. Influence of obesity on load-transfer mechanism, contact mechanics, and longevity of cemented acetabular cup. J Orthop. 2024;55:118–23.
39. Kumar A, Ghosh R, Kumar R. Effect of Implant Materials on Bone Remodelling Around Cemented Acetabular Cup. In: *4th International and 19th National Biennial Conferences on Machines and Mechanisms (iNaCoMM): Dec 07–07 2019; Indian Inst Technol Mandi, Suran, INDIA*; 2019: 17–26.


## Publisher's note